Activation of the ATPase Activity of Adeno-Associated Virus Rep68 and Rep78†

Susan S. Dignam,‡ John J. Correia,§ Shadia E. Nada,‡,|| James P. Trempe,‡ and John David Dignam*,‡

Department of Biochemistry and Cancer Biology, University of Toledo College of Medicine, 3035 Arlington Avenue, Toledo, Ohio 43614-5804, and Department of Biochemistry, University of Mississippi Medical Center, 2500 North State Street, Jackson, Mississippi 39216

Received November 21, 2006; Revised Manuscript Received March 13, 2007

ABSTRACT: Rep68 and Rep78 DNA helicases, encoded by adeno-associated virus 2 (AAV2), are required for replication of AAV viral DNA in infected cells. They bind to imperfect palindromic elements in the inverted terminal repeat structures at the 3′- and 5′-ends of virion DNA. The ATPase activity of Rep68 and Rep78 is stimulated up to 10-fold by DNA containing the target sequence derived from the inverted terminal repeat; nontarget DNA stimulates ATPase activity at 50-fold higher concentrations. Activation of ATPase activity of Rep68 by DNA is cooperative with a Hill coefficient of 1.8 ± 0.2. When examined by gel filtration at 0.5 M NaCl in the absence of DNA, Rep68 self-associates in a concentration-dependent manner. In the presence of DNA containing the binding element, Rep68 (and Rep78) forms protein−DNA complexes that exhibit concentration-dependent self-association in gel filtration analysis. The ATPase activity of the isolated Rep68−DNA and Rep78−DNA complexes is not activated by additional target DNA. Results of sedimentation velocity experiments in the presence of saturating target DNA are consistent with Rep68 forming a hexamer of the protein with two copies of the DNA element. Activation of the ATPase activity of Rep68 is associated with the formation of a protein−DNA oligomer.

Adeno-associated virus 2 (AAV2) is a nonpathogenic member of the parvoviridiae (*1*, *2*) that requires helper functions provided by another virus (*3*−*6*), such as adenovirus, to replicate efficiently and produce infectious virions. Because it is nonpathogenic and can integrate specifically at a site on chromosome 19 (*7*−*9*), AAV2 has attracted attention as a potential gene therapy vector (*10*−*13*). The genome encodes the capsid proteins, VP1, VP2, and VP3, and four replication proteins, Rep40, Rep52, Rep68, and Rep78. Rep68 and Rep78 have a 225 residue N-terminal structure that is absent in Rep40 and Rep52 and is responsible for DNA sequence specific binding (*14*). The N-terminal structure results from translation of a longer mRNA transcribed from the p5 promoter. Shorter mRNAs for Rep40 and Rep52 are transcribed from the p19 promoter. Rep68 and Rep40 differ from Rep78 and Rep52 at their C-termini as a result of alternate splicing, which replaces a 92 amino acid residue element in Rep78 and Rep52 with a 9 residue element in Rep68 and Rep40. All four proteins have DNA helicase and ATPase activities while only Rep68 and Rep78 exhibit a site-specific nuclease (*15*) and specific binding to the inverted terminal repeat element (ITR) at the 5′- and 3′-ends of the virion DNA. The sequence-specific binding and endonuclease activities reside in the 225 residue N-terminal element, which can recognize the target sequence independently of the rest of the protein (*16*). Rep68 or Rep78 is required to create the primer used in replication by cleaving the ITR while Rep40 and Rep52 are important for efficient packaging of the single-stranded genomic DNA into virions (*17*, *18*).

Rep68 and Rep78 are classified as SF3 helicases based on the organization and sequence of conserved sequence motifs (*19*) and the crystal structure of the C-terminal domains (*20*). Like other helicases (*21*−*23*), Rep68 and Rep78 couple energy from the hydrolysis of ATP to the unwinding of duplex nucleic acids with 3′ to 5′ polarity (*24*). Most DNA helicases exist as oligomers or assemble into oligomers on DNA or upon binding a nucleotide; Rep68/78 (*25*) also forms oligomers on target DNAs. In some instances the proteins are monomeric in the absence of DNA but function as dimers, as is the case with the Rep (*26*−*28*) and UvrD (*29*, *30*) helicases of *Escherichia coli*. Others exist as preformed oligomers, as is the case with the RepA helicase required for replication of plasmid RSF1010 (*31*−*34*) and the DnaB protein of *E. coli* (*35*), though the latter requires magnesium ions for oligomerization. Some hexameric helicases, including the T7 (*36*, *37*) and T4 (*38*) bacteriophage enzymes and SV40 large T-antigen (*39*, *40*), require a nucleotide for oligomerization. While helicases functioning as monomers has not been ruled out, and was proposed for the Rep and UvrD of *E. coli* (*41*, *42*), oligomerization is a feature of most helicases and may be linked to their function as motor proteins. Association of monomers to oligomers may be stabilized by the ligand. Analysis of the interaction of helicases with ligands requires determination of the nature of the oligomeric state of the protein and rigorous evaluation of the solution conditions required for oligomerization.

† This work was supported by National Institutes of Health Grants AI51471 and GM64765 (to J.P.T.) and National Institutes of Health Shared Instrumentation Grant PAR-02-036. This is manuscript 44 from the UMMC Analytical Ultracentrifuge Facility.

* Corresponding author. Phone: 419-383-4136. Fax: 419-383-6228. E-mail: David.Dignam@utoledo.edu.

‡ University of Toledo College of Medicine.

§ University of Mississippi Medical Center.

|| Present address: Department of Biology, University of Toledo, Toledo, OH.

10.1021/bi602412r CCC: $37.00
Published on Web 05/03/2007

AAV2 Rep68 and Rep78 form oligomers when they bind to DNA, though the exact oligomeric state is uncertain. A hexameric structure was proposed in one study based on the behavior of a Rep78−DNA complex on size exclusion chromatography and on the size of products in chemical cross-linking experiments (*43*). Multiple species in gel mobility shift experiments also suggest multiple oligomeric states (*44*). In other studies investigators proposed that the enzyme forms a dimer based on the enzyme concentration dependence of helicase activity (*25*). Because the oligomeric state of Rep68 and Rep78 is likely an important feature of their function as helicases, we have conducted critical studies of the oligomerization of these proteins and the solution conditions required for activation of their ATPase activity by the target DNA.

EXPERIMENTAL PROCEDURES

Materials. NADH, phosphoenolpyruvate, ATP, lactate dehydrogenase, and pyruvate kinase were obtained from Sigma. [γ-^{32}P]ATP (from MP Biomedicals) used for ATPase assays was applied to a 0.25 mL column of Q-Sepharose in 20 mM Tris-HCl (pH 7.5) and eluted with the same buffer containing 0.5 M NaCl; this step was required to remove Norit A nonadsorbable radioactive material that contributed to a high blank in the assay. Chromatographic media (Q-Sepharose, S-Sepharose, Sephacryl S300, and Superose 12) were from GE Healthcare. Ni-NTA Superflow was from Qiagen. Common laboratory salts and reagents were obtained from various suppliers.

Purification of Rep68His. Rep68His was expressed in *E. coli* (SG13009) harboring plasmid pStump68; this plasmid contains the coding sequence for Rep68 in a plasmid (pQE70; Qiagen) designed for inducible expression in bacteria (*45*). Cells were grown in LB, supplemented with M9 salts, 1% glucose, 25 μg/mL kanamycin, and 100 μg/mL ampicillin (*46*) at 37 °C to an A_{600} of 0.8 to 1; IPTG was added to 0.2 mM, and cells were harvested after 3 h and stored frozen at −70 °C. Preparation of the extract and Ni-NTA chromatography were performed at 0−4 °C. Partially thawed cell pellets (40−50 g) were suspended with a Dounce homogenizer (A pestle) in 6 volumes of 50 mM Tris-HCl (pH 7.5 at 25 °C), 10% (v/v) glycerol, 0.1% (v/v) Triton X-100, 2 mM EDTA, 1 mM dithiothreitol, 1 mM phenylmethanesulfonyl fluoride, and 0.01 mg/mL egg white lysozyme. NaCl and $MgCl_2$ were added with stirring to 0.5 M and 5 mM, respectively, and the extract was stirred for 30 min. The extract was subjected to centrifugation for 30 min at 20000g_{av}. Polyethylene glycol 8000 [0.25 volume of a 50% (w/v) solution] was added, with stirring, to the supernatant and stirred for 30 min. The precipitate was collected by centrifugation (20000g_{av}, 30 min) and dissolved in 30−40 mL of 20 mM Tris-HCl (pH 7.5), 20% (v/v) glycerol, and 0.5 M NaCl with a Dounce homogenizer (A pestle). The sample was applied to a 5 mL column of Ni-NTA Superflow (Qiagen) equilibrated in the same buffer. The column was washed with 10 column volumes of starting buffer and eluted successively with 5 column volumes each of buffer containing 0.05 and 0.4 M imidazole; Rep68 was in the 0.4 M imidazole eluate. Fractions were assayed for ATPase activity and examined by SDS−polyacrylamide gel electrophoresis; Rep68-containing fractions were pooled, dithiothreitol (to 0.5 mM) and EDTA (to 0.2 mM) were added, and the material was concentrated to 2−3 mL with Vivaspin 6 mL concentrators (Vivascience; 10000 MWCO). The concentrated material was applied as 0.5 mL aliquots to a Superose 12 gel filtration column (1 cm × 32 cm; GE Healthcare) equilibrated in 20 mM Tris-HCl (pH 7.5), 10% (v/v) glycerol, 0.5 M NaCl, 0.5 mM DTT, 2 mM $MgCl_2$, and 0.2 mM EDTA. Chromatography was performed at room temperature at 0.5 mL/min; fractions were collected and immediately placed on ice. Fractions were assayed for ATPase activity and examined by SDS−polyacrylamide gel electrophoresis (see Figure 1); Rep68-containing fractions from multiple runs were combined, concentrated, and stored frozen at −70 °C.

Purification of Untagged Rep68. E. coli BL21(DE3) Rosetta (Novagen) cells harboring a plasmid encoding Rep68 without the polyhistidine tag (pRep68, in pET9a) were grown as described for the His-tagged protein. Cells (20 g) were extracted and subjected to PEG fractionation as described for the His-tagged protein. The 0−10% PEG fraction was applied to Q-Sepharose (20 mL bed volume) equilibrated in 20 mM Tris-HCl (pH 7.5), 20% (v/v) glycerol, 100 mM NaCl, 0.5 mM DTT, and 0.2 mM EDTA. Rep68 eluted in the unbound fraction and active fractions were combined; 0.25 volume of 5 M NaCl was added to a final concentration of 1 M and applied to phenyl-Sepharose equilibrated in 25 mM Tris-HCl (pH 7.5), 1 mM EDTA, 10% (v/v) glycerol, 1 mM DTT, and 1 M ammonium sulfate. The column was washed with starting buffer and eluted successively with buffer containing 0.75, 0.5, and 0.25 M ammonium sulfate; Rep68 eluted in the 0.75 and 0.5 M fractions. Active fractions were combined and concentrated to 0.7 mL using Vivaspin 6 mL concentrators (10000 MWCO). The concentrated material was applied to Superose 12 equilibrated in 20 mM Tris-HCl (pH 7.5), 10% (v/v) glycerol, 250 mM NaCl, 0.5 mM DTT, and 0.2 mM EDTA; Rep68 eluted at the retention time of thyroglobulin. Active fractions were pooled, concentrated to 0.5 mL, and applied to the same Superose 12 column equilibrated with buffer containing 0.5 M NaCl. Active fractions under these conditions eluted at the retention time of IgG.

Purification of MBPRep78. Rep78 was expressed in *E. coli* as a maltose binding protein (MBP) fusion encoded by a plasmid (pRepmal78) (*47*, *48*). Cells were grown at 37 °C in LB medium containing M9 salts (*46*), 2 mM $MgSO_4$, 0.1 mM $CaCl_2$, 1% (w/v) glucose, and 50 μg/mL ampicillin to an A_{600} of 0.8 to 1.0 and induced with 0.2 mM IPTG. Cells were grown for 3 h after induction and harvested by centrifugation. Purification procedures were performed at 4 °C. Cells (25 g in a typical preparation) were suspended in 5 volumes of 25 mM Tris-HCl (pH 7.5 at 25 °C), 1 mM EDTA, 1 mM DTT, 20% (v/v) glycerol, 250 mM NaCl, 0.1% (v/v) Triton X-100, 1 mM PMSF, and 0.01 mg/mL lysozyme and incubated 30 min. The extract was centrifuged at 27000g_{av} for 30 min, and the supernatant was retained. Polyethylene glycol (MW 8000) was added slowly to 10% (w/v) with stirring to the supernatant fraction by the addition of 0.25 volume of a 50% (w/v) solution; the sample was stirred for 30 min after the PEG was added. The suspension was centrifuged at 17000g_{av} for 40 min, and the precipitate was suspended with a Dounce homogenizer (A pestle) in 50 mL of buffer A [25 mM Tris-HCl (pH 7.5 at 25 °C), 0.5 mM EDTA, 1 mM DTT, 20% (v/v) glycerol, 50 mM NaCl, and 1 mM PMSF]. The solution was applied to a Q-

Sepharose column (2.5 × 10.5 cm) equilibrated with the same buffer, and the column was washed with 4 bed volumes of the same buffer. The column was eluted with a 20 volume linear gradient from 50 mM to 1 M NaCl in buffer A. Fractions were assayed for ATPase activity and examined by SDS gel electrophoresis, and MBPRep78-containing fractions were combined and concentrated with an Amicon ultrafiltration cell using a PM10 membrane. The concentrated material was applied to a Sephacryl S-300 gel filtration column (1.5 × 141 cm) equilibrated in 25 mM Tris-HCl, pH 7.5, 0.5 mM EDTA, 1 mM DTT, 20% (v/v) glycerol, and 200 mM NaCl and eluted at 10 mL/h. Fractions were examined by enzyme assays and by SDS−PAGE, pooled, diluted to 50 mM NaCl, and applied to a column of S-Sepharose (1.5 × 15 cm) equilibrated in 25 mM Tris-HCl (pH 7.5), 0.5 mM EDTA, 1 mM DTT, 20% (v/v) glycerol, and 50 mM NaCl. The column was eluted at 30 mL/h with a 10 column volume gradient of NaCl from 50 to 400 mM. Fractions were assayed for ATPase and examined by SDS−PAGE, and active fractions were stored at −80 °C.

ATPase Assays. ATPase activity was determined spectrophotometrically by coupling the production of MgADP to the pyruvate kinase and lactate dehydrogenase reactions (*49*, *50*). Reaction mixtures contained 50 mM Tris-HCl (pH 7.5), 5 mM $MgCl_2$, 50 mM NaCl, 0.1 mg/mL bovine serum albumin, 1 mM MgATP, 1 mM phosphoenolpyruvate, 0.2 mM NADH, 25 units/mL pyruvate kinase, and 29 units/mL lactate dehydrogenase. Reactions were initiated by the addition of Rep68, and absorbance at 340 nm was monitored in a Beckman DU640 spectrophotometer equipped with a temperature controller. Temperature was maintained at 30 °C. Activity was determined from the change in absorbance at 340 nm, using the extinction coefficient for NADH of 6.22 mM^{-1} cm^{-1}. In some experiments ATPase activity was determined by a radioactive, stopped time assay. The stopped time assay was performed in 25 μL reactions containing 50 mM Tris-HCl (pH 7.5), 50 mM NaCl, 2 mM $MgCl_2$, 0.2 mM [γ-^{32}P]ATP (20−50 cpm/pmol), 1% (v/v) glycerol, and enzyme. Reactions were incubated for 10 min at 30 °C and stopped with 15 μL of 15% (w/v) perchloric acid and 50 μL of a 12.5% (w/v) Norit A suspension in water. The mixture was centrifuged in a microcentrifuge at 14000 rpm for 10 min, 20 μL of the supernatant was spotted on a 1.5 cm square of Whatman 1 filter paper, the papers were dried, and radioactivity was determined by liquid scintillation counting. One unit is the amount of enzyme that hydrolyzes 1 nmol of ATP to ADP and P_i per minute.

Determination of Extinction Coefficients. The UV spectrum of MBPRep78 was recorded from 210 to 350 nm on a sample dialyzed for 17 h against buffer A without DTT using the dialysis buffer for the reference. Absorbance at 205 nm was determined to calculate the extinction coefficient at 280 nm (*51*). The absorbance coefficient at 280 nm for the MBPRep78 was 10.6 for a 1% solution. The absorbance coefficient at 280 nm for the Rep68 was calculated from composition (*52*) and was 16 for a 1% solution. Molar extinction coefficients for Rep68 at 260 and 280 nm were respectively 6.57×10^4 M^{-1} cm^{-1} and 9.958×10^4 M^{-1} cm^{-1}.

Sucrose Gradient Velocity Sedimentation. Rep68 or MBPRep78 (7−15 μM) and A-stem (15−30 μM) in 25 mM Tris-HCl, pH 7.5, 100 mM NaCl, 5 mM magnesium acetate, 2 mM EDTA, and 2 mM DTT were incubated for 30 min on ice and diluted in the same buffer without NaCl. Samples of 100 μL were loaded on 2 mL gradients of 6−20% (w/v) sucrose in 25 mM Tris-HCl, pH 7.5, 50 mM NaCl, 1 mM EDTA, and 1 mM DTT. Rep68 (7.6 μM) without DNA in the same buffer with 500 mM NaCl was loaded onto a sucrose gradient containing 500 mM NaCl. Samples of MBPRep78 were applied to gradients with 50 mM NaCl. Molecular weight markers, catalase ($S_{20,w}$ 11.3, MW 250000), alcohol dehydrogenase ($S_{20,w}$ 7.4, MW 141000), and hemoglobin ($S_{20,w}$ 4.3, MW 64500), in the same buffer were loaded on a separate gradient; molecular weights indicated parenthetically for the markers are for their oligomeric molecular weights. The gradients were centrifuged in a TLS-55 rotor in a Beckman TLX ultracentrifuge at 180000g_{av} for 5.5 h at 4 °C and fractionated from the top. Fractions were assayed for ATPase activity, in the absence or presence of DNA, and analyzed by SDS gel electrophoresis. Catalase (*53*) and alcohol dehydrogenase (*54*) were assayed spectrophotometrically, and hemoglobin was determined spectrophotometrically from its absorbance at 418 nm. Molecular weights were calculated from $S_{20,w}$ and $D_{20,w}$ (from the R_s determined by size exclusion chromatography) as described in refs *55* and *56*.

Glutaraldehyde Cross-Linking of Rep68His. Rep68His or untagged Rep68 (0.5 mg mL^{-1}) in 20 mM HEPES−NaOH (pH 7.5), 2 mM $MgCl_2$, and 0.5 mM DTT was incubated with or without A-stem DNA and at various NaCl concentrations and 0.005% glutaraldehyde for 10 min at 22 °C. The reaction was quenched by the addition of sample buffer for SDS gel elctrophoresis. Samples were analyzed on 6% or 10% acrylamide−bisacrylamide SDS gels.

Size Exclusion Chromatography. Samples of Rep68 and the Rep68−A-stem complex were prepared as described for the sucrose density gradients, and 100 μL samples were chromatographed on a Phenomenex BioSep-SEC-3000 column (4.6 × 300 mm, fractionation range 5000−700000 Da) equilibrated with 20 mM Tris-HCl, pH 7.5, 0.2 mM EDTA, 1 mM DTT, 2 mM $MgCl_2$, and 100 mM NaCl (Rep68−A-stem complex) or 500 mM NaCl (Rep68). The flow rate was 0.5 mL/min, and absorbance was monitored at 280 nm (Rep68 and standards) or 260 nm (Rep68−A-stem complex). Gel filtration standards from Bio-Rad contained thyroglobulin (MW 670000, R_s 85 nm), bovine γ-globulin (MW 158000, R_s 5.1 nm), chicken ovalbumin (MW 44000, R_s 3.2 nm), equine myoglobin (MW 17000, R_s 2.3 nm), and vitamin B_{12} (MW 1350); molecular weights indicated parenthetically are for the oligomers. Fractions of Rep68 and the Rep68−A-stem complex were analyzed as for the sucrose gradients. The concentration dependence of the size of Rep68 was determined by diluting protein in 25 mM Tris-HCl (pH 7.5), 500 mM NaCl, 5 mM $MgCl_2$, 0.2 mM EDTA, and 0.5 mM DTT to 100, 60, 30, 12, and 6 μM. Samples of 50 μL were chromatographed on a Phenomenex BioSep-SEC-3000 column equilibrated in the same buffer. To determine the concentration dependence of the size of the Rep68−A-stem complex, Rep68 was combined with a 2-fold molar excess of A-stem in 25 mM Tris-HCl, pH 7.5, 5 mM $MgCl_2$, 0.2 mM EDTA, 0.5 mM DTT, and 100 mM NaCl. The sample was concentrated in a Vivaspin 2 mL centrifugal concentrator to 60 μM Rep68. The concentrated sample was diluted with the same buffer containing 100 mM NaCl to 30, 12, 6, 3,

and 1.5 μM, and 50 μL samples were chromatographed on a Phenomenex BioSep-SEC-3000 column equilibrated in the same buffer.

Analytical Ultracentrifugation. The complex of A-stem and Rep68 was prepared as described for sucrose gradients and gel filtration. In some experiments samples were subjected to chromatography on Superose 12 to remove free A-stem and used for sedimentation velocity experiments. Samples used in experiments performed in the presence of excess A-stem were applied to Sephadex G-50 fine spin columns equilibrated in 20 mM Tris-HCl (pH 7.5), 2 mM $MgCl_2$, 0.2 mM EDTA, 0.5 mM DTT, and 50 or 100 mM NaCl. Sedimentation velocity experiments were performed at two or three concentrations in a Beckman XLA analytical ultracentrifuge (Beckman Coulter Inc., Fullerton, CA) equipped with absorbance optics using an An60Ti rotor. Sedimentation velocity data were converted to a distribution of sedimentation coefficients [$c(s)$ vs S] with Sedfit and analyzed by direct boundary fitting to discrete assembly models using SedAnal (*57*). Samples were centrifuged at 35000 rpm at 3.6 °C, and sample cells were scanned at 280 and 260 nm. Extinction coefficient data used for global analysis were as follows: for A-Stem at 260 nm, 23 mL mg^{-1} cm^{-1}, and at 280 nm, 11.9 mL mg^{-1} cm^{-1}; for Rep68 at 260 nm, 0.927 mL mg^{-1} cm^{-1}, and at 280 nm, 1.606 mL mg^{-1} cm^{-1}. Multiple wavelength data are useful for estimating stoichiometry and verifying discrete models in direct boundary fitting (SedAnal). The partial specific volume of Rep68 calculated from composition was 0.732 cm^3 g^{-1}, and the calculated subunit molecular weight was 61876 (Sednterp) (*58*). The partial specific volume of A-stem DNA was taken as 0.55 cm^3 g^{-1} with a calculated molecular weight of 16578. Sedimentation coefficient data were converted to $S_{20,w}$ using density and viscosity values calculated with Sednterp.

SDS−Polyacrylamide Gel Electrophoresis. Samples were treated with SDS (1%) and mercaptoethanol (5%) and subjected to electrophoresis on 10% acrylamide−bisacrylamide (30:1) gels (*59*) and stained with Coomassie blue R250.

Preparation of Oligonucleotides. Duplex oligonucleotides were prepared by mixing equimolar concentrations of complementary oligonucleotides in 20 mM Tris-HCl (pH 7.5 at 25 °C), 100 mM NaCl, and 1 mM EDTA, heating to 100 °C for 5 min, and cooling slowly (over 3−5 h) to room temperature (*60*). The sequences of the oligonucleotides were as follows: A-stem-1, 5′-GATCTCAGTGAGCGAGCGAGCGCGCA- 3′; A-stem-2, 5′-GATCTGTGCGCGC TCGCTCGCTCACTGA-3′; Ala-1, 5′-TAAGGATTTCTTCAATCTTAGGATCGGCCA-3′; Ala-2, 5′-TAGGCCGATCCTAAGATTGAAGAAATCT-3′. A-stem is the duplex formed from A-stem-1 and A-stem-2, and NC30 is the duplex formed from Ala-1 and Ala-2. The extinction coefficients for duplex A-stem at 260 and 280 nm were respectively 4.317×10^5 and 1.98×10^5 M^{-1} cm^{-1}.

RESULTS

Purification of Rep68His and MBPRep78. The studies described in this work required quantities of Rep68His and MPBRep78 sufficient for biophysical studies that were free of activities that interfere with analysis of the ATPase activity. Rep68His was purified from cell extracts by polyethylene glycol fractionation, chromatography on a Ni-chelate resin, and HPLC gel filtration, and ATPase was monitored in the absence or presence of an oligonucleotide (A-stem) containing the recognition sequence from the AAV2 ITR (*61*, *62*). Chromatography on Superose 12, shown in Figure 1, was essential for removal of contaminating DNA bound to the protein that interfered with analysis of activation of ATPase activity. Performing the purification in high salt was necessary for the His-tagged protein because it precipitates reversibly at low ionic strength and moderate protein concentrations; untagged Rep68 and MBPRep78 are soluble at low ionic strength. The complex of Rep68His with A-stem DNA is soluble at low ionic strength. Rep68 without the polyhistidine was purified by precipitation with polyethylene glycol, ion-exchange chromatography, hydrophobic chromatography, and gel filtration. While the ATPase activity was similar to Rep68His, it did not precipitate at low ionic strength. However, it exhibits concentration-dependent association at low ionic strength in the absence of the target DNA. The DNA-independent and DNA-dependent ATPase activities in the elution profile are coincident with the peak of protein. MBPRep78 was purified by a combination of ion-exchange and gel filtration column chromatography. We resorted to conventional purification procedures since only a fraction of MPBRep78 (10−20%) in extracts bound to amylose resin employed for purification of maltose binding protein fusions. Material eluting with maltose was contaminated with other proteins and interfering nonspecific phosphatase activity. Unlike Rep68His, free MBPRep78 without DNA containing the binding element is soluble at low ionic strength. The ATPase activity of MBPRep78 was also stimulated by DNA, and the DNA-stimulated ATPase and DNA-independent ATPase activities were also coincident in the elution profile in the last S-Sepharose chromatographic step (data not shown). MBPRep78 was used as a fusion protein since the maltose binding protein fusion was resistant to digestion with factor Xa.

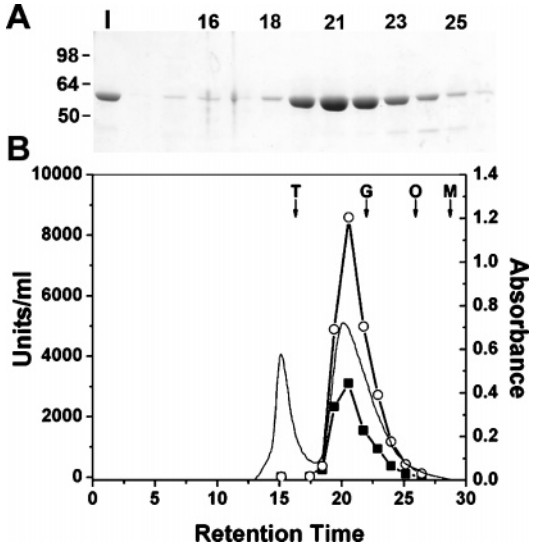

FIGURE 1: Superose 12 purification of Rep68. Pooled, concentrated fractions from the Ni-NTA step were applied to Superose 12. (A) SDS−PAGE of Superose 12 fractions. I, concentrated Ni-NTA pool; fractions are indicated by retention time. The positions of molecular weight standards are indicated. (B) Absorbance at 295 nm (—); ATPase activity in the absence (●) or presence (○) of 125 nM A-stem. Molecular weight standards: T, thyroglobulin, 670000; G, bovine γ-globulin, 158000; O, ovalbumin, 44000; M, myoglobin, 17000.

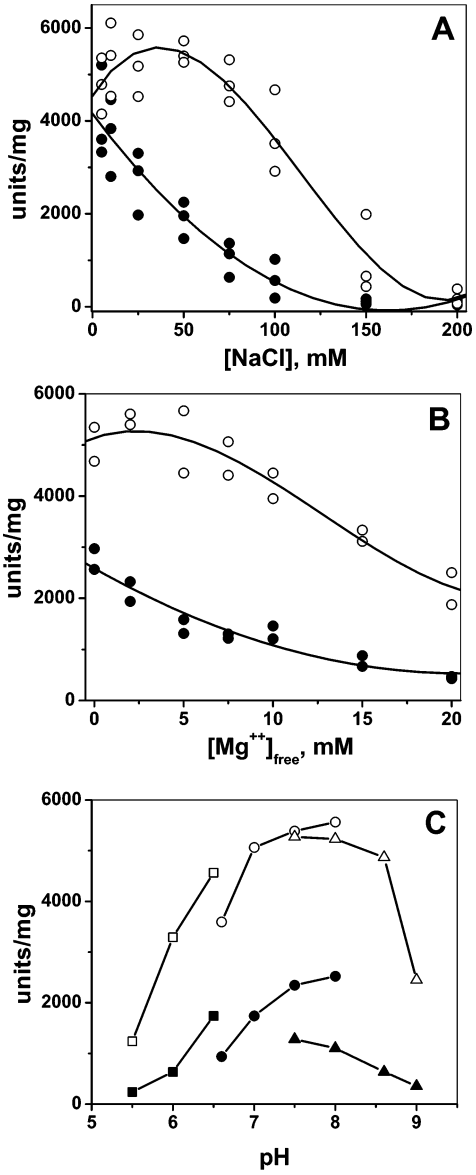

FIGURE 2: Effect of ionic strength, free Mg^{2+}, and pH on ATPase activity and activation by DNA. The concentrations of Rep68 and A-stem were 25 nM in all assays. (A) ATPase assays were performed at the indicated concentrations of NaCl in the absence (●) or presence (○) of A-stem with 5 mM $MgCl_2$ and 50 mM Tris-HCl (pH 7.5). The lines are the fit of a polynomial to data from three experiments. (B) ATPase assays were performed at the indicated concentrations of free Mg^{2+} ($MgCl_2$) in the absence (●) or presence (○) of A-stem. NaCl was 60 mM at 0 $MgCl_2$ and was adjusted to maintain constant ionic strength at the higher $MgCl_2$ concentrations; the buffer was 50 mM Tris-HCl (pH 7.5). The lines are the fit of a polynomial to data from two experiments. (C) ATPase assays were performed at the indicated pH values in the absence (closed symbols) or presence (open symbols) of A-stem. Buffers were 50 mM MES−NaOH (■, □), 50 mM HEPES−NaOH (●, ○), and 50 mM Tris-HCl (▲, △). NaCl was 50 mM with Tris-HCl (7.5), $MgCl_2$ was 5 mM, and the ionic strength was kept constant with the other buffers by adjusting NaCl concentration.

Characterization of the DNA-Activated ATPase Activity. We examined solution conditions for the ATPase activity of Rep68His and MBPRep78 as shown in Figure 2. As shown in panel A, the ionic strength optima for the A-stem stimulated and the unstimulated ATPase activities were different. At low ionic strength, there was little stimulation by A-stem DNA, while the highest stimulation was observed at 75 mM NaCl. The absence of activation at low ionic strength may be related to reversible association of the protein at low salt. High ionic strength prevents binding of DNA to Rep68, and this effect probably accounts for the small activation by DNA and reduced activity at high salt. As shown in panel B, the magnitude of activation is also influenced by magnesium ion concentration (2-fold at 0 free magnesium and 4-fold at 15 mM free magnesium), though the effect is less dramatic than that of NaCl. The choice of buffer and the pH of the reaction also influenced the degree of activation as shown in panel C. The effect of NaCl, $MgCl_2$, and pH were also examined with MBPRep78 with similar results (not shown). The results show that activation of the ATPase activity is strongly influenced by solution conditions which affect both binding to DNA and the oligomeric state of the protein.

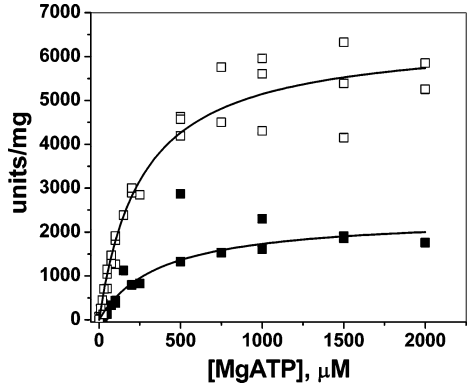

FIGURE 3: Determination of apparent K_{MgATP} and V_{max} for Rep68. ATPase assays were performed at the indicated concentrations of MgATP in the absence (■) or presence (□) of A-stem. The lines are the fit to a hyperbolic function of two (minus A-stem) or three (plus A-stem) separate experiments.

Table 1: Kinetic Parameters of Rep68 and MBPRep78[a]

	K_{MgATP}, μM	V_{max}, units/mg
Rep68His minus A-stem	370 ± 90	2400 ± 200
Rep68His plus A-stem	260 ± 35	6500 ± 300
MBPRep78 minus A-stem	600 ± 100	200 ± 60
MBPRep78 plus A-stem	240 ± 50	790 ± 100

[a] Data were fit to a hyperbolic function as described for Figure 3. Results are shown ± the standard deviation of the fit.

Kinetic Constants for ATPase Activity. We examined the dependence of ATPase activity on [MgATP] as shown in Figure 3 for Rep68His. Activity showed a hyperbolic dependence on the concentration of the nucleotide. Similar studies were performed with MBPRep78 (not shown), and the results were similar to those for Rep68His; the results for Rep68His and MBPRep78 are summarized in Table 1.

Activation of ATPase Activity by DNA. The concentration dependence of activation of Rep68His by DNA at two concentrations of enzyme was examined as shown in Figure 4A. The enzyme was activated up to 8-fold, showing a sigmoidal dependence of activity on A-stem concentration, consistent with cooperative binding of the ligand. Values for K_{A-stem} were 2.4 ± 0.1 nM at 25 nM Rep68 and 3.8 ± 0.3 nM at 40 nM Rep68; the Hill coefficient was 1.7 ± 0.1 at 25 nM Rep68 and 1.8 ± 0.1 at 40 nM Rep68. Maximum activation occurred at substoichiometric concentrations of A-stem with respect to Rep68His. Nontarget oligonucleotides of similar size and composition gave little activation at the concentrations of A-stem employed in the experiments shown

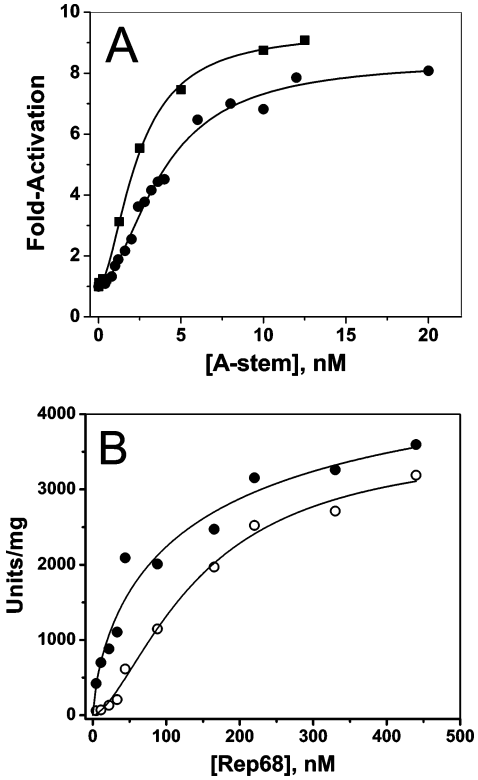

FIGURE 4: Dependence of activation of ATPase activity on concentration of A-stem and Rep68. Panel A: ATPase assays were performed at the indicated concentrations of A-stem. The concentrations of Rep68 were 25 nM (■) and 40 nM (●). Panel B: ATPase assays were performed at the indicated concentrations of Rep68 in the presence (●) or absence (○) of 1 μM A-stem. The lines are fits of the Hill equation to the data.

in Figure 4, indicating that activation is sequence specific. Micromolar concentrations of a 30 base pair nontarget DNA activated severalfold, and the DNA removed during purification by chromatography of Rep68His on Superose 12 also activated at high concentrations. Similar results were obtained with MBPRep78. Activation did not depend on the nature of the assay since similar results were obtained with a coupled spectrophotometric assay and a stopped time assay measuring the release of PO_4^{3-} from [γ-^{32}P]ATP. Activation at saturating A-stem also shows a marked dependence on enzyme concentration as shown in Figure 4B. Much higher activation (7−10-fold) is seen at low enzyme concentrations, and activity is higher in the presence or absence of saturating A-stem at higher enzyme concentrations. The enzyme concentration dependence of activation and enzyme activity is consistent with the association of inactive subunits into more active oligomers. These results for activation of Rep68His by DNA differ significantly from those of Zhou et al. (*24*), who saw little activation (1.4-fold) of the ATPase activity by an oligonucleotide containing the Rep binding element. The difference between our results and those of Zhou et al. (*24*) may reflect differences in the enzyme preparations, enzyme concentrations, and the sensitivity of the activity to solution conditions; the activity and activation of the enzyme are affected by ionic strength, and these earlier studies were done without NaCl in the assay.

To analyze the specificity of the DNA activation, we examined the effect of duplex and single-stranded target (A-stem) on ATPase activity; four different enzyme preparations were examined, and a data set from one example is presented

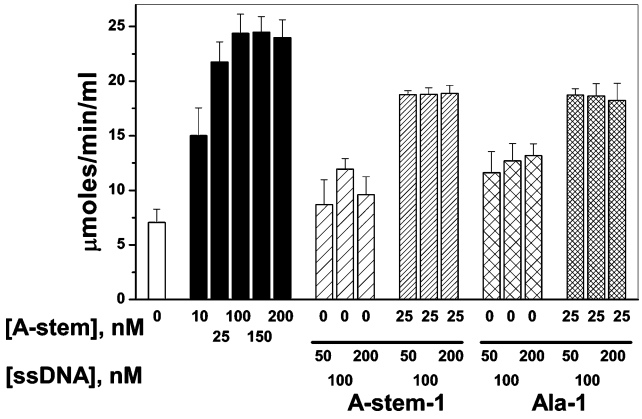

FIGURE 5: Activation of Rep68 by different DNAs. Rep68 (50 nM) was assayed for ATPase activity in the presence of the indicated concentrations of A-stem (duplex). ATPase assays were also performed at the indicated concentrations of single strand DNAs in the absence or presence of 25 nM A-stem. A-stem-1: a 26 base oligonucleotide from the Rep target sequence. Ala-1: a 30 base oligonucleotide of an unrelated sequence. Results are the mean ± SD of three experiments.

in Figure 5. Duplex A-stem DNA activated ATPase from 3- to 9-fold (3.5-fold in the example in Figure 5), with maximal activation at substoichiometric concentrations with respect to Rep68. Single-stranded DNA (A-stem-1) used for duplex A-stem and an unrelated single-stranded oligonucleotide of approximately the same size (Ala-1) gave little activation even at high concentrations. Activation by duplex A-stem was not significantly affected by the target or nontarget single-stranded DNA in the experiment presented in Figure 5. With some enzyme preparations the single strands at high concentrations antagonized activation. Nontarget duplex DNA (N30) gave little activation (~1.4-fold) at 100 nM (not shown). Maximal activation by DNA, in addition to being sequence specific, requires duplex structure. We also examined the effect of target and nontarget DNA on the ATPase activity of Rep78Mal and obtained qualitatively similar results (i.e., activation by the target A-stem and little activation by single strands or nontarget duplex DNA).

Characterization of the Rep−Target DNA Complex. To understand how the target DNA activates Rep68His and MBPRep78, we examined the size of the free proteins and their complexes formed with DNA by gel filtration and sucrose density gradient centrifugation. Figure 6 shows the results of such experiments for Rep68His. In the absence of DNA the protein elutes from a size exclusion column (panel A) at a size slightly larger than the monomer molecular weight; the ATPase is activated approximately 8-fold by A-stem DNA. Later experiments show that the retention time is concentration dependent. Rep68His without DNA was run in high salt (0.5 M NaCl) since it precipitated at low ionic strength (below 200 mM NaCl). When Rep68His was examined by sucrose density gradient centrifugation (panel B), the protein sedimented at a position close to hemoglobin and was activated by A-stem DNA approximately 5-fold. A complex of Rep68 and A-stem was also examined by gel filtration (Figure 6, panel A) and sucrose density gradient centrifugation (Figure 6, panel B). We obtained similar results with the untagged form of Rep68; the untagged protein did not precipitate at low ionic strength. In both gel filtration and sedimentation experiments, Rep68 with A-stem elutes as a larger species that is not activated by A-stem

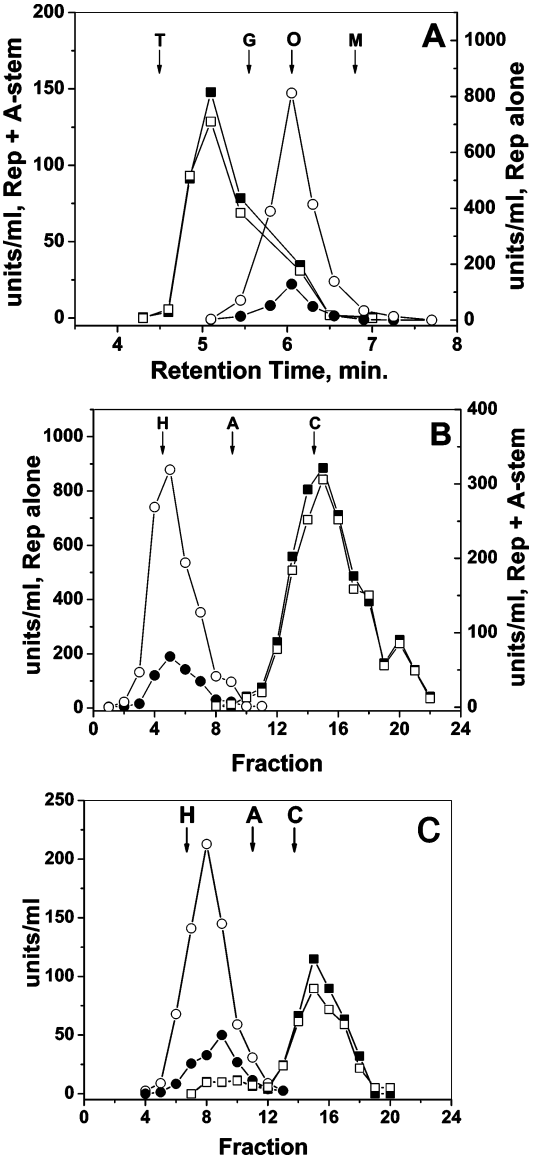

FIGURE 6: Determination of the size of Rep68 and of the complex of Rep68 with A-stem. (A) The complex of Rep68His formed with A-stem (squares) or free Rep68His without A-stem (circles) was fractionated on a size exclusion column (Phenomenex BioSep-SEC-3000). Fractions were assayed for ATPase activity in the absence (■, ●) and presence (□, ○) of additional A-stem. Molecular weight standards: T, thyroglobulin, 670000, R_s 8.5 nm; G, bovine γ-globulin, 158000, R_s 5.1 nm; O, ovalbumin, 44000, R_s 3.2 nm; M, myoglobin, 17000, R_s 2.3 nm. (B) The complex of Rep68His formed with A-stem (squares) or Rep68 alone (circles) was fractionated on 5−20% (w/v) sucrose gradients. Fractions were assayed for ATPase activity in the absence (●, ■) and presence (○, □) of A-stem. Molecular weight standards: H, hemoglobin, 64500, $S_{20,w}$ 4.3; A, alcohol dehydrogenase, 141000, $S_{20,w}$ 7.4; C, catalase, 252000, $S_{20,w}$ 11.3. (C) MBP-Rep78 combined with A-stem (squares) or MBP-Rep78 alone (circles) was fractionated on 5−20% (w/v) sucrose gradients. Fractions were assayed for ATPase activity in the absence (●, ■) and presence (○, □) of A-stem.

DNA. A-stem DNA was well resolved from the protein in both separation methods so that the absence of activation reflects the presence of DNA in the complex. Unlike free Rep68His, the Rep68His−DNA complex remained in solution at relatively low ionic strength; the complex was dissociated from DNA by high ionic strength, precluding analysis of the free Rep68 and Rep68−DNA complex under the same ionic strength. On both size exclusion chromatography and sucrose density gradient centrifugation, the behavior of the complex suggested that it was not homogeneous with respect to size since the peaks are broad; on sucrose density gradients (see panel B in Figure 6), the peak of activity was at approximately 11.6 s with clear evidence of larger species. We also examined MBPRep78 by sucrose density gradient centrifugation and gel filtration and obtained results similar to those obtained with Rep68His, except that MBPRep78 did not precipitate at low ionic strength, allowing for examination of the free and DNA-bound forms under the same solution conditions. An example of results obtained for MBPRep78 on sucrose gradient sedimentation is shown in panel C of Figure 6; as with Rep68His, the ATPase activity of the free protein was activated by A-stem while the ATPase activity of the complex was not. As is shown later in gel filtration experiments, both the free protein and the Rep68−A-stem complex show concentration-dependent self-association.

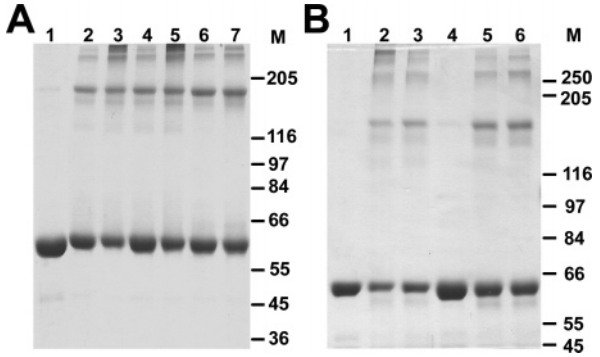

FIGURE 7: Glutaraldehyde cross-linking of Rep68. (A) SDS−acrylamide gel (10%) electrophoresis of cross-linked Rep68His: (1) no cross-linking; (2) cross-linking at 50 mM NaCl with A-stem; (3) cross-linking at 50 mM NaCl without A-stem; (4) cross-linking at 100 mM NaCl with A-stem; (5) cross-linking at 100 mM NaCl without A-stem; (6) cross-linking at 500 mM NaCl with A-stem; (7) cross-linking at 500 mM NaCl without A-stem. (B) SDS−acrylamide gel (6%) electrophoresis of cross-linked Rep68His and untagged Rep68: (1) Rep68His, no cross-linking; (2) Rep68His, cross-linking at 100 mM NaCl without A-stem; (3) Rep68His, cross-linking at 100 mM NaCl with A-stem; (4) Rep68 untagged, no cross-linking; (5) Rep68 untagged, cross-linking at 100 mM NaCl without A-stem; (6) Rep68 untagged, cross-linking at 100 mM NaCl with A-stem.

Cross-Linking Studies. We examined the association of Rep68His by using glutaraldehyde to covalently cross-link oligomeric species. As shown in Figure 7 (panel A, 10% acrylamide, and panel B, 6% acrylamide), incubation with glutaraldehyde produced a species with a mobility corresponding to approximately 180000; this species is consistent with a trimer of the subunits (185568 predicted from sequence). If cross-linking was performed at low ionic strength, in the absence of A-stem (lanes 3 and 5 in panel A and lane 2 in panel B), larger cross-linked material was detected. The amount of these species were far less when A-stem was present (lanes 2 and 4 in panel A and lane 3 in panel B). There are also at least two larger species that may correspond to oligomers of the trimer. When these experiments were performed at low protein concentrations (not shown) or high ionic strength (panel A, lanes 6 and 7), the amount of the larger species was reduced. Similar results were obtained with Rep68 lacking the His tag (panel B, lanes 5 and 6), except that the level of high molecular weight material was far less at low ionic strength, consistent with

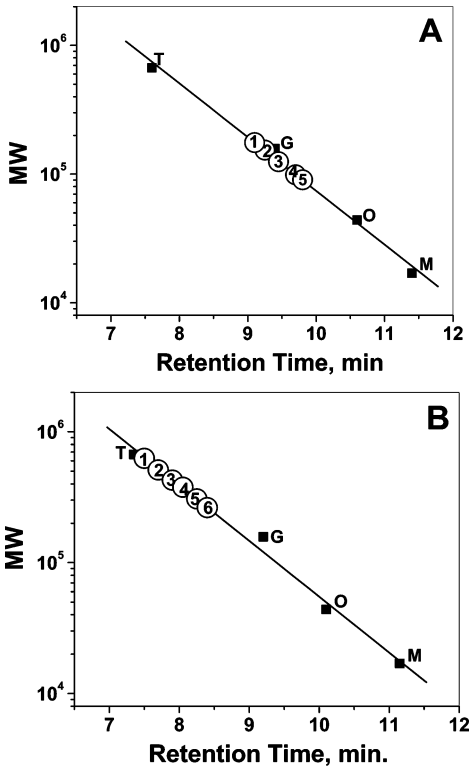

FIGURE 8: Concentration dependence of the size of Rep68His and of the complex of Rep68His with A-stem. (A) Rep68His was applied to a SEC column at 60, 30, 12, and 6 μM (2−5). A sample of the concentrated Ni-NTA pool, estimated at 100 μM (1), was also applied. Molecular weight standards are as described for Figure 1. Estimated molecular weights: 1, 176000; 2, 154000; 3, 125000; 4, 99000; 5, 90400. (B) Rep68His was combined with A-stem to form a complex and applied to a SEC column at 60, 30, 12, 6, 3, and 1.5 μM (1−6). Estimated molecular weights: 1, 627000; 2, 511000; 3, 428000; 4, 377000; 5, 307000; 6, 263000.

this protein showing less tendency to precipitate under these conditions. Similar-sized cross-linked species are seen with both the untagged and His-tagged versions of Rep68 in the presence of DNA, suggesting that these species seen with the tagged protein do not reflect an effect of the tag.

Concentration-Dependent Self-Association of Rep68His. We characterized the properties of the free protein and the Rep68His−A-stem complex in more detail to obtain estimates of size. The concentration dependence of the retention time of Rep68His on gel filtration chromatography in 0.5 M NaCl indicates that it undergoes reversible self-association as shown in Figure 8A. This result indicates that the protein forms oligomers in the absence of DNA. The tendency of the protein to oligomerize is more pronounced at low ionic strength, to the point that it precipitates below 200 mM NaCl. At the lowest loading concentration, the protein eluted at a retention time between those expected for a dimer and a monomer. At 0.25 M NaCl the protein remains in solution but is aggregated, eluting ahead of thyroglobulin when examined by gel filtration. The Rep68His−A-stem complex showed behavior indicative of self-association (Figure 8, panel B) but was significantly larger, giving approximately 260000 for the apparent molecular weight at the lowest protein concentration examined (6 μM) with values approaching 630000 at the highest protein concentration examined (60 μM). The ATPase activity of the complex in all cases was independent of added A-stem. When samples of the large species obtained at high Rep68His concentrations (60 μM) were rechromatographed on the same column, the peak of the complex eluted at a retention time indicative of reversible dissociation of an oligomer into a smaller species corresponding to those seen at lower loading concentrations.

Analytical Ultracentrifugation. We examined the Rep68His−A-stem complex by sedimentation velocity to obtain an estimate of its size by a rigorous method that is independent of standards. In some experiments the complex was examined without free A-stem DNA while in others there was excess free DNA. The cells were scanned at 260 and 280 nm to determine the distribution of the complex and the A-stem DNA. The results of these studies are shown in Figure 9. Panels A and B show the distribution of sedimentation coefficients [presented as $c(s)$ vs S] for several experiments done in (A) 50 mM NaCl and (B) 100 mM NaCl. The insert in both panels is an enlargement of the complex region of the distribution. Data collected at 260 and 280 nm give very close agreement consistent with a tight complex comprised of two A-stem per six Rep68 subunits. Figure 9C presents the weight average S values for regions of the $c(s)$ distributions corresponding to free A-stem DNA and the Rep68−A-stem complex from several experiments. There is reasonable agreement between the different salt concentrations and the presence or absence of excess A-stem DNA. In the absence of a significant excess of free A-stem the Rep68−A-stem complex exhibits a tendency to aggregate into large species consistent with the tendency of the free protein to precipitate. This latter observation might also reflect the formation of higher order oligomers as suggested by band shift assays in work by Owens et al. (*63*). In the presence of excess A-stem the complex tends to sediment as a well-defined species (see inserts in Figure 9A,B). The best extrapolated S value for the 2:6 complex in both salt concentrations is 13.15 $S_{20,w}$ as indicated by the vertical line in the inserts. The tendency of the complex to adsorb to surfaces or precipitate during the exchanging of buffers during sample preparation precluded examination of higher complex concentrations; this was particularly true at 50 mM NaCl. Free A-stem sedimented at 3.28 ± 0.22 $S_{20,w}$, consistent with a MW value of 16578 based on the sequence. At higher concentrations A-stem sediments in a concentration-dependent manner consistent with weak self-association due to complementary overhang regions.

DISCUSSION

Oligomerization of AAV2 Rep68. DNA helicases serve an essential function in the replication of both cellular and viral genomes. The large replication proteins of AAV2, Rep68 and Rep78, serve important roles in viral replication by creating the site for the initiation of DNA replication by nicking a site in the ITR through an endonuclease activity in the N-terminal domains and then acting as a helicase with 3′ to 5′ polarity. Though the mechanism of neither the bacterial nor the eukaryotic helicases is entirely understood, they function as motor proteins, coupling energy derived from the hydrolysis of ATP to the separation of DNA strands. In their function as motor proteins, oligomeric structure is an important feature. *E. coli* Rep helicase and related helicases of Gram-negative bacteria have been proposed to function as dimers with the two subunits binding alternately to duplex and single-stranded DNA in what has been called the rolling model; an alternate view is that they function as

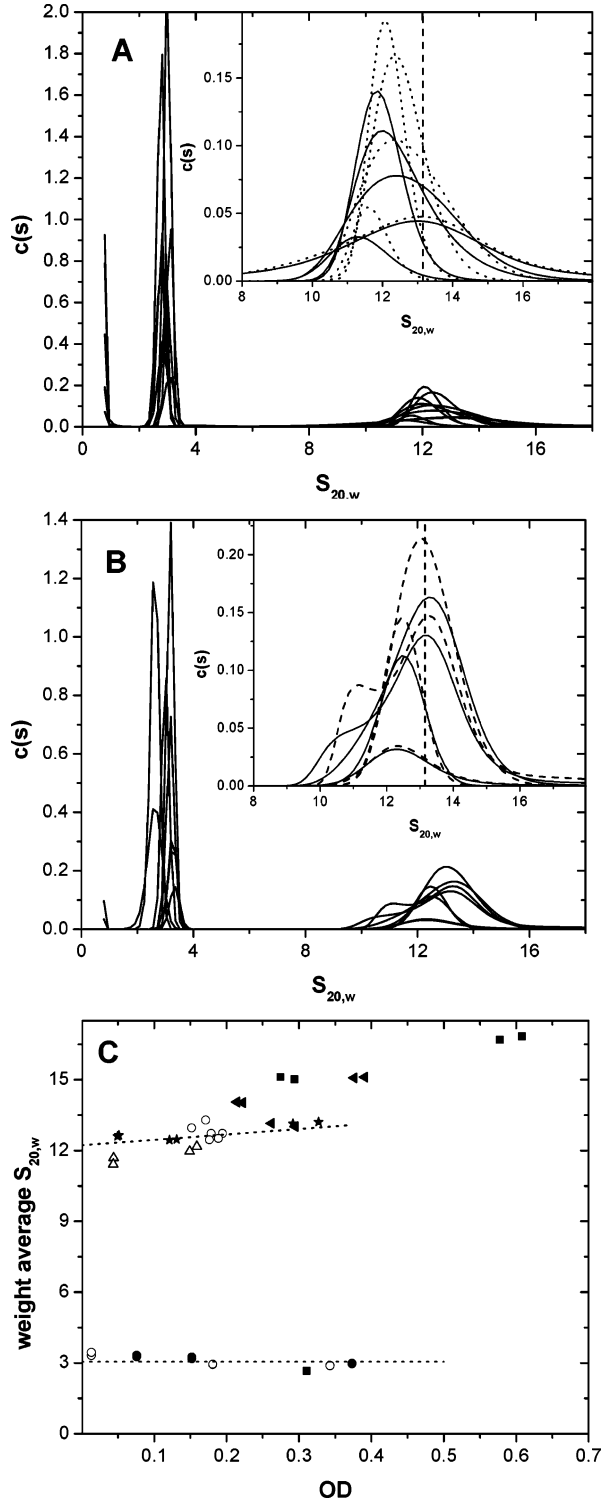

FIGURE 9: Sedimentation velocity of the Rep68−A-stem complex. Panel A: The distribution of sedimentation coefficients [shown as $c(s)$ vs $S_{20,w}$] for experiments in standard buffer conditions plus 50 mM NaCl. Panel B: $c(s)$ vs $S_{20,w}$ for experiments in standard buffer conditions plus 100 mM NaCl. The inserts in (A) and (B) enlarge the region of the distribution corresponding to the A-stem−Rep68 heterocomplex; vertical lines correspond to 13.15 $S_{20,w}$. Solid lines are data collected at 280 nm; dotted lines are data collected at 260 nm. Panel C: Concentration dependence of weight average $S_{20,w}$ vs OD corresponding to integration of the free A-stem or the heterocomplex region of the distribution. Open symbols correspond to 50 mM NaCl and closed symbols to 100 mM NaCl. The different symbols correspond to data from different experiments. The upper line reflects the trend of the heterocomplex $S_{20,w}$ data in excess A-stem, and the lower line reflects the average A-stem $S_{20,w}$.

monomers akin to an inchworm. The hexameric helicases are either stable oligomers or form hexamers on their DNA substrates; in some cases the association is promoted by ATP. Our analysis of AAV2 Rep68 indicates that it forms oligomers on the target DNA from the AAV2 ITR, consistent with a hexameric helicase. An $S_{20,w}$ of 12.22 to 13.15 $S_{20,w}$ for the Rep68−A-stem complex is consistent with six subunits of Rep68 and two copies of the target DNA. Analysis of the Rep68−A-stem complex by gel filtration indicates that it undergoes concentration-dependent self-association; the size of the species seen at low protein concentrations is consistent with the results of analytical ultracentrifugation. The data are most consistent with the formation of a hexameric structure that associates reversibly to form larger oligomeric species. The biological significance of these larger species is unclear since they are seen at high protein concentrations. However, some of the species detected in electrophoretic mobility shift assays may correspond to different oligomeric states of the complex.

Activation of AAV2 Rep68 ATPase. An important feature of Rep68 is its ATPase activity, which is required both for the helicase function and to open the DNA at the site of the endonucleolytic cleavage in the ITR. The ATPase activity is stimulated by DNA and is associated with oligomerization of the protein. The association with oligomerization suggests that a conformational transition, linked to formation of oligomers, activates the ATPase. The monomers may have low intrinsic ATPase activity that is enhanced by oligomerization, or the enzyme may be inactive as a monomer with the activation reflecting the equilibrium distribution between inactive monomer and active oligomer. In either case, binding to target DNA would shift the distribution toward the more active oligomer. In the absence of the target DNA, dissociation of the oligomer and reduction in ATPase activity are also favored by low protein concentration and high ionic strength.

Structural Relationship of Rep68 and Rep78 to Other DNA Helicases. The AAV2 Rep helicases belong to the SF3 class of helicases, and most members of this group form hexameric ring-like structures. One early report suggested that Rep78 also formed a hexamer (*43*), though the data supporting this proposition were not as extensive as the data presented here. Our results are consistent with a hexameric model but could include trimers and species larger than a hexamer detected in the glutaradehyde cross-linking experiments. We did not see significant effects when the cross-linking was performed in the presence of ATP or ATPγS, indicating that, unlike SV40 T-antigen, assembly does not require the nucleotide. However, the nucleotide might alter affinity of the protein for DNA as suggested by effects on binding of Rep68 to the AAV2 ITR detected in band shift assays (*44*, *64*). Effects of nucleotides have precedent in the SV40 T-antigen (*39*, *40*) and some phage helicases (*36*−*38*) whose oligomerization is stimulated by ATP.

While no crystal structures have been reported for Rep68 or Rep78, structures were determined for the N-terminal nuclease/DNA binding domain (*65*) present in Rep68 and Rep78 and for Rep40 (*20*, *66*). The Rep40 structure was determined on the free protein (*20*) and on a complex with ADP (*66*). Although Rep40 was not crystallized as an oligomer in these studies, based on the similarity of the structure to SV40 T-antigen and other AAA+ proteins (*67*)

it was modeled as a hexamer (*20*). Presumably Rep68 and Rep78 have the potential to form similar structures since they likely have some of the same surfaces for protein−protein interaction present in Rep40. We do see evidence of large oligomers by gel filtration, by sucrose gradient sedimentation, and by glutaraldehyde cross-linking. While the most abundant species in cross-linking experiments appears to be a trimer, this species may form oligomers corresponding to a hexamer. SV40 T-antigen assembles into hexamers and double hexamers (*68*−*71*), but it also forms dimers and trimers that may be on a path leading to hexamers and double hexamers. Hexameric (*65*), trimeric (*72*), and dimeric oligomeric (*73*) forms were detected with the bovine papilloma virus (BPV) E1 protein, a homologue of SV40 T-antigen. Oligomerization of SV40 T-antigen and BPV E1 is affected by ATP and DNA, and EM reconstructions (*71*) and X-ray structures of SV40 T-antigen (*70*) suggest that oligomerization is coupled to ligand binding. Analysis of multiple oligomeric forms of Rep68 and Rep78 complexes by electrophoretic mobility shift assays indicates that one or two copies of the ITR (*62*) bind to various oligomeric forms and ATP promotes the formation of some of these oligomeric species (*44*). Effects of ATP are also seen with the binding of NS1 of minute virus of mice, the MVM equivalent of Rep68 and Rep78, to the MVM replication origins (*74*). Although Rep78 has been reported to form a hexamer on the stem of the ITR based on gel filtration and chemical cross-linking (*43*), the oligomeric state of the protein in these studies was not rigorously characterized. The ITR−Rep78 complex's behavior on gel filtration in these studies was consistent with a hexamer, but the amount of DNA bound was not determined. A case can be made for Rep68, Rep78, and Rep40 all forming hexamers, but the evidence supporting this idea is not entirely convincing at present, particularly with Rep40. The formation of an oligomer could involve a number of intermediate species that may depend on the presence of both the target sequence and nucleotide with the final active oligomeric form having limited stability; in such a case (i.e., Rep40), detection of the active oligomer would be difficult.

ACKNOWLEDGMENT

The authors thank Drs. Samuel Young and Jude Samulski for the Rep68His expression vector, Dr. Robert Kotin for the MBPRep78 expression vector, and Jacob Bieszczad for the construction of the untagged Rep68 expression vector. The authors acknowledge the helpful comments of an anonymous reviewer.

REFERENCES

1. Bloom, M. E., and Young, N. S. (2001) Parvoviruses, in *Fields Virology* (Knipe, D. M., and Howley, P. M., Eds.) 4th ed., Vol. 2, pp 2361−1379, Lippincott, Williams, & Wilkins, Baltimore, MD.
2. Muzyczka, N., and Berns, K. I. (2001) Parvoviridiae: the viruses and their replication, in *Fields Virology* (Knipe, D. M., and Howley, P. M., Eds.) 4th ed., Vol. 2, pp 2327−2359, Lippencott, Williams, & Wilkins, Baltimore, MD.
3. Liu, C., et al. (2001) Long-term localized transgene expression in the pancreas achieved by intra-arterial adenoassociated virus-mediated gene transfer, *Transplant. Proc. 33* (1−2), 603.
4. Georg-Fries, B., et al. (1984) Analysis of proteins, helper dependence, and seroepidemiology of a new human parvovirus, *Virology 134*, 64−71.
5. Berns, K. I., and Bohensky, R. A. (1987) Adeno-associated viurses: an update, *Adv. Virus Res. 32*, 243−306.
6. Schlehofer, J. R., Ehrbar, M., and zur Hausen, H. (1986) Vaccinia virus, herpes simplex virus, and carcinogens induce DNA amplification in a human cell line and suppport replication of a helper virus dpendent parvovirus, *Virology 152*, 110−117.
7. Kotin, R. M., et al. (1990) Site-specific integration by adeno-associated virus, *Proc. Natl. Acad. Sci. U.S.A. 87*, 2211−2215.
8. Cheung, A. K., et al. (1980) Integration of the adeno-associated virus genome into cellular DNA in latently infected human Detroit 6 cells, *J. Virol. 33*, 739−748.
9. Giraud, C., Winocour, E., and Berns, K. I. (1994) Site-specific integration by adeno-associated virus is directed by a cellular DNA sequence, *Proc. Natl. Acad. Sci. U.S.A. 91*, 10039−10043.
10. Owens, R. A. (2002) Second generation adeno-associated virus type 2-based gene therapy systems with the potential for preferential integration into AAVS1, *Curr. Gene Ther. 2*, 145−159.
11. Wright, J. F., et al. (2003) Recombinant adeno-associated virus: formulation challenges and strategies for a gene therapy vector, *Curr. Opin. Drug Discovery Dev. 6*, 174−178.
12. Buning, H., et al. (2003) AAV-based gene transfer, *Curr. Opin. Mol. Ther. 5*, 367−375.
13. Hermonat, P. L., and Muzyczka, N. (1984) Use of adeno-associated virus as a mammalian DNA cloning vector: transduction of neomycin resistance into mammalian tissue culture cells, *Proc. Natl. Acad. Sci. U.S.A. 81*, 6466−6470.
14. Owens, R. A., et al. (1993) Identification of a DNA-binding domain in the amino terminus of adeno-associated virus Rep proteins, *J. Virol. 67*, 997−1005.
15. Im, D. S., and Muzyczka, N. (1990) The AAV origin binding protein Rep68 is an ATP-dependent site-specific endonuclease with DNA helicase activity, *Cell 61*, 447−457.
16. Cathomen, T., Collete, D., and Weitzman, M. D. (2000) A chimeric protein containing the N terminus of the adeno-associated virus Rep protein recognizes its target site in an in vivo assay, *J. Virol 74*, 2372−2382.
17. Dubielzig, R., et al. (1999) Adeno-associated virus type 2 protein interactions: Formation of pre-encapsidation complexes, *J. Virol. 73*, 8989−8998.
18. Chejanovsky, N., and Carter, B. J. (1989) Mutagenesis of an AUG codon in the adeno-associated virus rep gene: effects on viral DNA replication, *Virology 173*, 120−128.
19. Tuteja, N., and Tuteja, R. (2004) Unraveling DNA helicases. Motif, structure, mechanism and function, *Eur J. Biochem. 271*, 1849−1863.
20. James, J. A., et al. (2003) Crystal structure of the SF3 helicase from adeno-associated virus type 2, *Structure (Cambridge) 11*, 1025−1035.
21. von Hippel, P. H., and Delagoutte, E. (2001) A general model for nucleic acid helicases and their "coupling" within macromolecular machines, *Cell 104*, 177−190.
22. Delagoutte, E., and von Hippel, P. H. (2002) Helicase mechanisms and the coupling of helicases within macromolecular machines. Part I: Structures and properties of isolated helicases, *Q. Rev. Biophys. 35*, 431−478.
23. Caruthers, J. M., and McKay, D. B. (2002) Helicase structure and mechanism, *Curr. Opin. Struct. Biol. 12*, 123−133.
24. Zhou, X., et al. (1999) Biochemical characterization of adeno-associated virus rep68 DNA helicase and ATPase activities, *J. Virol. 73*, 1580−1590.
25. Weitzman, M. D., et al. (1996) Interaction of wild-type and mutant adeno-associated virus (AAV) Rep proteins on AAV hairpin DNA, *J. Virol. 70*, 2440−2448.
26. Wong, I., et al. (1996) ATPase activity of *Escherichia coli* Rep helicase is dramatically dependent on DNA ligation and protein oligomeric states, *Biochemistry 35*, 5726−5734.
27. Wong, I., and Lohman, T. M. (1997) A two-site mechanism for ATP hydrolysis by the asymmetric Rep dimer P2S as revealed by site-specific inhibition with ADP-A1F4, *Biochemistry 36*, 3115−3125.
28. Cheng, W., et al. (2001) *E. coli* Rep oligomers are required to initiate DNA unwinding in vitro, *J. Mol. Biol. 310*, 327−350.
29. Maluf, N. K., Fischer, C. J., and Lohman, T. M. (2003) A dimer of *Escherichia coli* UvrD is the active form of the helicase in vitro, *J. Mol. Biol. 325*, 913−935.
30. Maluf, N. K., Ali, J. A., and Lohman, T. M. (2003) Kinetic mechanism for formation of the active, dimeric UvrD helicase-DNA complex, *J. Biol. Chem. 278*, 31930−31940.

31. Roleke, D. (1997) Crystallization and preliminary X-ray crystallographic and electron microscopic study of a bacterial DNA helicase (RSF1010 RepA), *Acta Crystallogr., Sect. D: Biol. Crystallogr. 53* (Part 2), 213−216.
32. Niedenzu, T., et al. (2001) Crystal structure of the hexameric replicative helicase RepA of plasmid RSF1010, *J. Mol. Biol. 306*, 479−487.
33. Xu, H., et al. (2003) Structure of DNA helicase RepA in complex with sulfate at 1.95 Å resolution implicates structural changes to an "open" form, *Acta Crystallogr., Sect. D: Biol. Crystallogr. 59* (Part 5), 815−822.
34. Jezewska, M. J., Galletto, R., and Bujalowski, W. (2004) Interactions of the RepA helicase hexamer of plasmid RSF1010 with the ssDNA. Quantitative analysis of stoichiometries, intrinsic affinities, cooperativities, and heterogeneity of the total ssDNA-binding site, *J. Mol. Biol. 343*, 115−136.
35. Bujalowski, W., Klonowska, M. M., and Jezewska, M. J. (1994) Oligomeric structure of *Escherichia coli* primary replicative helicase DnaB protein, *J. Biol. Chem. 269*, 31350−31358.
36. Patel, S. S., and Hingorani, M. M. (1993) Oligomeric structure of bacteriophage T7 DNA primase/helicase proteins, *J. Biol. Chem. 268*, 10668−10675.
37. Picha, K. M., and Patel, S. S. (1998) Bacteriophage T7 DNA helicase binds dTTP, forms hexamers, and binds DNA in the absence of Mg^{2+}. The presence of dTTP is sufficient for hexamer formation and DNA binding, *J. Biol. Chem. 273*, 27315−27319.
38. Gogol, E. P., et al. (1992) Cryoelectron microscopic visualization of functional subassemblies of the bacteriophage T4 DNA replication complex, *J. Mol. Biol. 224*, 395−412.
39. San Martin, M. C., Gruss, C., and Carazo, J. M. (1997) Six molecules of SV40 large T antigen assemble in a propeller-shaped particle around a channel, *J. Mol. Biol. 268*, 15−20.
40. Stenlund, A. (2003) Initiation of DNA replication: lessons from viral initiator proteins, *Nat. Rev. Mol. Cell Biol. 4*, 777−785.
41. Mechanic, L. E., Hall, M. C., and Matson, S. W. (1999) *Escherichia coli* DNA helicase II is active as a monomer, *J. Biol. Chem. 274*, 12488−12498.
42. Mechanic, L. E., Latta, M. E., and Matson, S. W. (1999) A region near the C-terminal end of *Escherichia coli* DNA helicase II is required for single-stranded DNA binding, *J. Bacteriol. 181*, 2519−2526.
43. Smith, R. H., Spano, A. J., and Kotin, R. M. (1997) The Rep78 gene product of adeno-associated virus (AAV) self-associates to form a hexameric complex in the presence of AAV ori sequences, *J. Virol. 71*, 4461−4471.
44. Li, Z., et al. (2003) Characterization of the adenoassociated virus Rep protein complex formed on the viral origin of DNA replication, *Virology 313*, 364−376.
45. Young, S. M., et al. (2000) Roles of adeno-associated virus Rep protein and human chromosme 19 in site-specific recombination, *J. Virol. 74*, 3953−3966.
46. Sambrook, J., E. F. F., and Maniatis, T. (1989) *Molecular Cloning: A laboratory manual*, Cold Spring Harbor Laboratory Press, Cold Spring Harbor, NY.
47. Chiorini, J. A., et al. (1994) Biologically active Rep proteins of adeno-associated virus type 2 produced as fusion proteins in *Escherichia coli*, *J. Virol. 68*, 797−804.
48. Wonderling, R. S., Kyostio, S. R., and Owens, R. A. (1995) A maltose-binding protein/adeno-associated virus Rep68 fusion protein has DNA-RNA helicase and ATPase activities, *J. Virol. 69*, 3542−3548.
49. Cleland, W. W. (1979) Optimizing coupled enzyme assays, *Anal. Biochem. 99*, 142−145.
50. Cook, P. F., et al. (1982) Adenosine cyclic 3′,5′-monophosphate dependent protein kinase: kinetic mechanism for the bovine skeletal muscle catalytic subunit, *Biochemistry 21*, 5794−5799.
51. Scopes, R. K. (1974) Measurement of protein by spectrophotometry at 205 nm, *Anal. Biochem. 59*, 277−282.
52. Gill, S. C., and von Hippel, P. H. (1989) Calculation of protein extinction coefficients from amino acid sequence data, *Anal. Biochem. 182*, 319−326.
53. Chance, B., Greenstein, D. S., and Roughton, F. J. (1952) The mechanism of catalase action. I. Steady-state analysis, *Arch. Biochem. 37*, 301−321.
54. Buhner, M., and Sund, H. (1969) Yeast alcohol dehydrogenase: SH groups, disulfide groups, quaternary structure, and reactivation by reductive cleavage of disulfide groups, *Eur. J. Biochem. 11*, 73−79.
55. Siegel, L. M., and Monty, K. J. (1966) Determination of molecular weights and frictional ratios of proteins in impure systems by use of gel filtration and density gradient centrifugation. Application to crude preparations of sulfite and hydroxylamine reductases, *Biochim. Biophys. Acta 112*, 346−362.
56. Siegel, L. M., and Monty, K. J. (1965) Determination of molecular weights and frictional ratios of macromolecules in impure systems: Aggregation of urease, *Biochem. Biophys. Res. Commun. 19*, 494−499.
57. Stafford, W. F., and Sherwood, P. J. (2004) Analysis of heterologous interacting systems by sedimentation velocity: curve fitting algorithms for estimation of sedimentation coefficients, equilibrium and kinetic constants, *Biophys. Chem. 108*, 231−243.
58. Laue, T. M., et al. (1992) *Analytical Ultracentrifugation in Biochemistry and Polymer Science* (Horton, J. C., Ed.) pp 90−125, Royal Society of Chemistry, Cambridge, England.
59. Laemmli, U. K. (1970) Cleavage of structural proteins during the assembly of the head of bacteriophage T4, *Nature 227*, 680−685.
60. Ren, J., et al. (1999) Spectral and physical characterization of the inverted terminal repeat DNA structure from adenoassociated virus 2, *Nucleic Acids Res. 27*, 1985−1990.
61. McCarty, D. M., et al. (1994) Identification of linear DNA sequences that specifically bind the adeno-associated virus Rep protein, *J. Virol. 68*, 4988−4997.
62. Weitzman, M. D., et al. (1994) Adeno-associated virus (AAV) Rep proteins mediate complex formation between AAV DNA and its integration site in human DNA, *Proc. Natl. Acad. Sci. U.S.A. 91*, 5808−5812.
63. Owens, R. A., et al. (1991) Adeno-associated virus rep proteins produced in insect and mammalian expression systems: wild-type and dominant-negative mutant proteins bind to the viral replication origin, *Virology 184*, 14−22.
64. Kyostio, S. R., Wonderling, R. S., and Owens, R. A. (1995) Negative regulation of the adeno-associated virus (AAV) P5 promoter involves both the P5 rep binding site and the consensus ATP-binding motif of the AAV Rep68 protein, *J. Virol. 69*, 6787−6796.
65. Hickman, A. B., et al. (2004) The nuclease domain of adeno-associated virus rep coordinates replication initiation using two distinct DNA recognition interfaces, *Mol. Cell 13*, 403−414.
66. James, J. A., et al. (2004) Structure of adeno-associated virus type 2 Rep40-ADP complex: insight into nucleotide recognition and catalysis by superfamily 3 helicases, *Proc. Natl. Acad. Sci. U.S.A. 101*, 12455−12460.
67. Hickman, A. B., and Dyda, F. (2005) Binding and unwinding: SF3 viral helicases, *Curr. Opin. Struct. Biol. 15*, 77−85.
68. Schuck, S., and Stenlund, A. (2005) Assembly of a double hexameric helicase, *Mol. Cell 20*, 377−389.
69. Gai, D., et al. (2004) Mechanisms of conformational change for a replicative hexameric helicase of SV40 large tumor antigen, *Cell 119*, 47−60.
70. Gai, D., et al. (2004) Insights into the oligomeric states, conformational changes, and helicase activities of SV40 large tumor antigen, *J. Biol. Chem. 279*, 38952−38959.
71. VanLoock, M. S., et al. (2002) SV40 large T antigen hexamer structure: domain organization and DNA-induced conformational changes, *Curr. Biol. 12*, 472−476.
72. Enemark, E. J., Stenlund, A., and Joshua-Tor, L. (2002) Crystal structures of two intermediates in the assembly of the papillomavirus replication initiation complex, *EMBO J. 21*, 1487−1496.
73. Sedman, J., and Stenlund, A. (1996) The initiator protein E1 binds to the bovine papillomavirus origin of replication as a trimeric ring-like structure, *EMBO J. 15*, 5085−5092.
74. Cotmore, S. F., et al. (1995) The NS1 polypeptide of the murine parvovirus minute virus of mice binds to DNA sequences containing the motif [ACCA]2-3, *J. Virol. 69*, 1652−1660.

BI602412R